CRYSTALLINE, HIBONITE-BEARING HASP CLASTS IN LUNAR METEORITE NORTHWEST AFRICA 2420. Paul H. Warren[1], K. D. McKeegan[1] N. Matsuda[1] and C. Ma[2], [1]EPS Science Department, UCLA, Los Angeles, CA 90095 USA, [2]Division Geol. Planetary Sci., California Inst. of Technology, Pasadena, CA 91125 USA

HASP (High-Alumina Silica-Poor matter: [1]) is a rare, intriguing material initially found among the glassy impact-spheroids scattered within lunar regolith samples. HASP is widely inferred to form as a result of evaporative loss of moderately volatile components, mainly FeO, MgO and SiO_2, from superheated droplets of shallow-crustal derivation launched within plumes of impact vapor [2,3,4]. An exception is Apollo 14 regolith breccia 14076, in which HASP occurs largely in the form relatively large and blocky chunks of a metastable Al_2O_3- and CaO-rich silicate mineral, yoshiokaite, for which [5] inferred an origin involving accumulation of molten HASP droplets into a thin surficial HASP-melt pool that cools slowly enough to allow the metastable yoshiokaite to form by devitrification, and yet fast enough to preserve yoshiokaite and not form the stable equivalent assemblage (likely, depending upon the detailed HASP composition, some combination of hibonite, corundum, anorthite and possibly gehlenite).

In a SEM survey of lithic diversity within lunar highland polymict breccia Northwest Africa (NWA) 2420, we discovered two extraordinarily Al_2O_3- and CaO-rich clasts. We initially suspected these might be remnants of chondritic CAI that survived accretion to the Moon (there is one precedent among lunar highland breccia clasts [6]). However, we utilized the UCLA ims-1290 ion probe to measure oxygen isotopes in the clasts, and found normal lunar-terrestrial $\delta^{18}O$ and more importantly $\Delta^{17}O$. Thus, neither clast is a CAI. They are new forms of lunar HASP. To better characterize these clasts, we acquired high-resolution backscattered electron images using the CalTech FE-SEM.

The two HASP clasts are 11 mm apart and are distinct in texture and mineralogy, but both are unlike previous HASP occurrences in that they consist mainly of stable, albeit very fine-grained, silicate minerals. The bigger of the two HASP clasts "A" is about 0.2 mm^2 and 0.66 mm in max dimension. The smaller HASP clast "B" is 0.10 mm in max dimension but only about 0.003 mm^2, in part because it has partially disaggregated and mixed with normal NWA 2420 material. However, the B clast is so extremely fine-grained and modally uniform (countless tiny grains of multiple minerals with no evidence of local modal heterogeneity) that 0.003 mm^2 may be an adequate sampling. Within clast A, there is clear modal heterogeneity.

Clast A consists of about 52 vol% plagioclase (An98), 36% gehlenite (almost pure, with MgO and FeO both averaging just 0.2 wt%), 7% hibonite (too fine-grained to be resolved by EPMA) and 5% Mg-Fe spinel (*mg* 62). Spinel occurs as scattered grains typically about 5-20 µm across. Gehlenite grains are typically 10-40 µm and somewhat clustered. Hibonite occurs as tiny lath-shaped grains, typically about 2×0.5 µm, severely clumped into several bands typically about 1 mm long and 0.1-0.2 mm wide (Fig. 1). Even in their centers these bands are not pure hibonite, but the ultra-fine interstitial material (plag?) is hard to characterize. Suspected hibonites, typically even narrower, also occur as inclusions within gehlenite and plag. By EPMA coupled with modal analysis, we estimate the bulk composition of clast A to be (in wt%) MgO 1.1, Al_2O_3 41.9, SiO_2 29.3, CaO 25.9, FeO 1.3, and TiO_2 ~ 0.17. The representativeness of this composition is likely compromised by the modal heterogeneity.

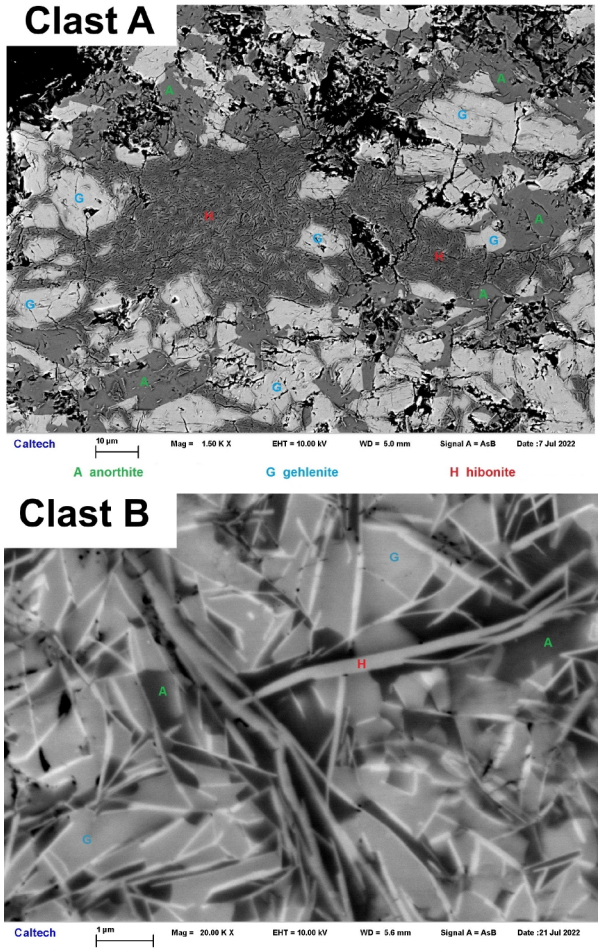

Fig. 1. Backscattered electron images.

Clast B is so extremely fine-grained (Fig. 1) its individual phases are impossible to analyze by EPMA. Compared to the A clast, B appears to have a similar hibonite content but a higher gehlenite/plag ratio. Gehlenite occurs as blocky grains typically about 1 µm across. Plagioclase is interstitial and even tinier by a factor of about 2. Intergrown with the gehlenite and plag is hibonite in the form of narrow laths and whiskers typically about 0.1 µm wide, but up to 6 µm long. The longest whiskers show curvature, a feature associated with crystallization involving, in addition to melt and solid(s), a vapor phase [7,8]. By simple averaging of 6 analyses, we estimate for clast B MgO 0.3, Al_2O_3 52, SiO_2 23, CaO 24.5, FeO 0.4, and TiO_2 ~ 0.07 wt%.

Like all other known HASP compositions, the two NWA 2420 clast compositions plot well to the high Al/Ca side of the gehlenite-hibonite boundary on the phase diagram of the system CaO-SiO_2-Al_2O_3 ([5], after [9]). Evolution of HASP composition was governed by melt-vapor equilibria [4] and not by crystal-melt equilibria. Crystalline HASP, as found in NWA 2420, could at least in principle undergo crystal-melt fractionations. But clast B is so ultra-fined grained it seems certain its nascent crystals never significantly separated from melt. The same cannot be said for the relatively coarse and heterogeneous clast A, but the expected first melt crystallization phase, hibonite, is also extremely fine grained in A.

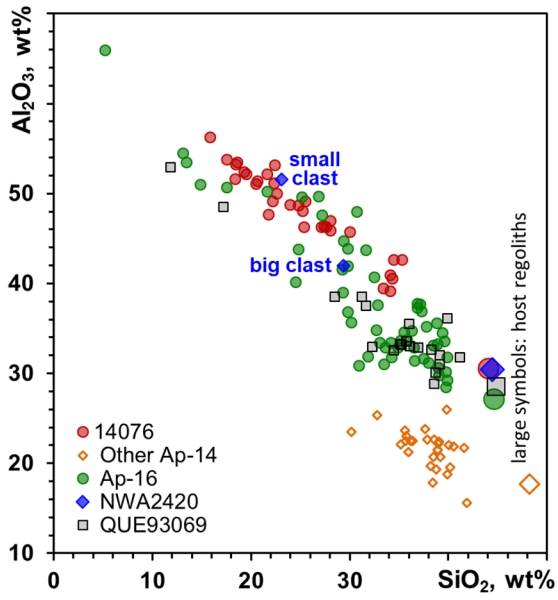

Fig. 2. SiO_2 and Al_2O_3 in 5 different HASP types.

As noted by [5], HASP suites show trends of enhancement of Al_2O_3 as a by-product of loss of SiO_2 (Fig. 2), and the Apollo 14 HASP suite shows evolution from the distinctly low-Al_2O_3 composition of the Apollo 14 highland regolith; which indicates that at least the Apollo 14 HASP formed locally, in a sub-basin-scale event. Our new data from NWA 2420 reinforce the distinctive nature of the Apollo 14 HASP. Data sources for Fig. 2 are too numerous to enumerate. All data from the QUE 93069 meteorite are our own [10]. The extreme composition with 66 wt% Al_2O_3 is from [11].

In the only previous modeling of crystalline HASP, [5] inferred that the 14076 metastable yoshiokaite formed in shallow surficial pools of landed still-molten HASP, cooling at a rate that favored devitrification at ~950-1200°C (for comparison, [4] inferred a peak temperature, for comparably extreme HASP, of ~1800°C). It was noted by [5] that a slower cooling rate, as expected for the interior of a somewhat thicker HASP-melt pool, might engender stable Ca-Al phases.

However, it is also conceivable that in the case of a relatively large impact event cooling and rapid, lathy crystallization might occur before HASP lands [cf. 12]. In the case of a suite of related condensate materials from 14076, apparently condensed near 1600°C [4], the texture of a large clast of the condensate material [3] suggests that droplets landed cool enough to largely survive as discrete, albeit condensate-melt-inundated, spheroids. As discussed by [3], the cooling history of materials entrained within an impact vapor plume would be sensitive to not only the flight length but also the complex dynamics of plume evolution, as the shielding provided by a cloud of opaque debris would serve to limit radiative cooling. The dainty hibonite-whisker texture of clast B would probably not survive a stage in which the material was suspended within a relatively thick and slow-cooling (compared to the yoshiokaite scenario) pool of superhot melt on the lunar surface.

The fate of impact vapor is an important yet poorly understood aspect of the Moon's cratering history. Each large-scale impact must have produced a massive vapor plume, and yet only scant deposits of either condensates or refractory (HASP) residues have been found. The crystalline HASP clasts of NWA 2420 go some slight ways toward reducing and constraining this deficit.

References: [1] Naney M.T. et al. (1976) *PLPSC, 7,* 155. [2] Papike J.J. et al. (1997) *Am. Mineral., 82,* 630. [3] Warren P.H. (2008) *GCA, 72,* 3562. [4] Yakovlev O.I. et al. (2011) *Geoch. Int., 49,* 211. [5] Vaniman D.T. & Bish D.L. (1990) *Am. Mineral., 75,* 676. [6] Joy K.H. et al. (2012) *Science, 336*, 1426. [7] Miyamoto M. et al. (1979) *Geochem. J., 13*, 1. [8] Gong W. et al. (2017) *Materials, 2017/10*, 1. [9] Levin E.M. et al. (1964) *Phase Diagrams for Ceramists*, 219–220. [10] Warren P.H. & Kallemeyn G.W. (1995) *LPS, XXV*, 1465. [11] Keller L.P. and McKay D.S. (1992) *PLPSC, 22*, 137. [12] Symes S.J. et al. (1998) *MaPS, 33,* 13.